

Supplementary Informations

Oxidation of Phospholipids by OH Radical Coordinated to Copper Amyloid- β Peptide—A Density Functional Theory Modelling

Alberto Rovetta, Laura Carosella, Federica Arrigoni, Jacopo Vertemara, Giuseppe Zampella, Luca De Gioia, Luca Bertini

Department of Biotechnologies and Biosciences, University of Milano-Bicocca, Piazza della Scienza 2, 20126 Milan, Italy. Email luca.bertini@unimib.it

Summary

1. DFT Speciation and structure of $\text{Cu}(\text{OH})_2^- \text{A}\beta(1-7)$ complexes. 2
2. DFT Speciation and structure of $\text{Cu}(\text{OH})_2^- \text{A}\beta(1-7)$ 1-methyl 2-methyl phosphatidylcholine adducts. 5
3. Structures of the $\text{Cu}(\text{II})(\text{OH})_2^- \cdot \text{A}\beta$ fat acid chain adducts. 9
4. NBO Spin charges of the final propagation product $\text{Cu}(\text{H}_2\text{O})(\text{OH}^-) \text{A}\beta \text{PC}$. 9
5. $\text{Cu}(\text{II})(\text{OH})_2^- \text{A}\beta \text{PC}$ PES scan of 4C and 5C in comparison. 11
6. Palmitic acid 16:0 reactivity with free solvated OH radical. 13

Table S1. DFT Optimized Cu(II)(OH)₂·Aβ(1-7) models. Aβ(1-7) is the DAEFRHD C-term acetylated capped peptide. The total net charge of this model is -1. E and ΔE refers to the total energy and the total energy difference computed with respect to the most stable isomer (1). The structures are then classified according to the Cu coordination number (CN) and the interaction between Arg5 guanidinium side chain with the other side chains and/or peptide bond carbonylic groups.

N	CN	Apical ligand	Arg5 interactions.	DFT Energy (Hartree)	ΔE kcal/mol
1	4	-	D1 2D7 OH	-4960,3455	0,0
2	4	-	E3, 2 D7	-4960,3357	6,1
3	5	H6	2 D7, OH, CO	-4960,335	6,6
4	5	NH D1	2 E3, D1, D7	-4960,3343	7,0
5	5	H6	2 E3, D1, D7	-4960,3276	11,2
6	4	-	2 D7, 2 D1, OH	-4960,3186	16,9
7	6	C=O D1, C=O D7	2 E3, D7	-4960,3173	17,7
8	4	-	2 E3, C=O H6, D7	-4960,315	19,1
9	5	H6	2 OH, 2 E3	-4960,3134	20,1
10	5	E3	OH, D1, 2 D7	-4960,3134	20,1
11	4	-	E3	-4960,3114	21,4
12	5	H6	2 E3	-4960,3087	23,1
13	4	-	2 E3, 2 D7	-4960,3074	23,9
14	5	E3	E3, C=O H6, D7	-4960,3042	25,9
15	4	-	2 E3, 1 D7	-4960,3031	26,6
16	5	D7	D7, E3	-4960,3024	27,1
17	4	-	2 OH, 2 E3, D7	-4960,3022	27,2
18	5	E3	2 E3	-4960,3009	28,0
19	4	-	OH, D1, 2 E3, C=O D7	-4960,299	29,2
20	4	-	D1, D7, 2 E3	-4960,2989	29,2
21	5	H6	C=O E3, E3, 2 D7	-4960,2982	29,7
22	4	-	OH, 2 D7, E3	-4960,2979	29,8
23	4	-	2 OH, 2 D7, E3	-4960,2974	30,2
24	5	H6	D7, 2 E3	-4960,2973	30,3
25	5	H6	OH, 2 D7	-4960,2971	30,4
26	4	-	2 D7, E3	-4960,2965	30,7
27	4	-	2 D7, 2 E3	-4960,2961	31,0
28	5	D7	D7, E3	-4960,2952	31,6
29	5	H6	D1, 2 E3	-4960,2944	32,0
30	5	C=O D1	2 D1, 2E3	-4960,2944	32,1
31	4	-	D7, D1, 2 E3	-4960,293	32,9
32	4	-	2 OH, 2 D7, E3	-4960,2929	33,0
33	5	H6	OH, D7, E3	-4960,2928	33,1
34	5	C=O D1	2 D7, 2 E3, C=O R5	-4960,2868	36,8
35	5	C=O D1	2 D7, 2 E3, C=O R5	-4960,2868	36,8
36	4	-	D7, D1, 2 E3	-4960,2852	37,8
37	4	-	D1, E3	-4960,2827	39,4
38	5	H6	2 D7, E3	-4960,2799	41,2
39	4	-	D1, 2 E3	-4960,2782	42,2
40	5	H6	D1, E3	-4960,2743	44,7

41	4	-	D1, E3, D7, OH	-4960,2682	48,5
42	5	C=O D1	E3, C=O H6, 2 D7	-4960,2506	59,5

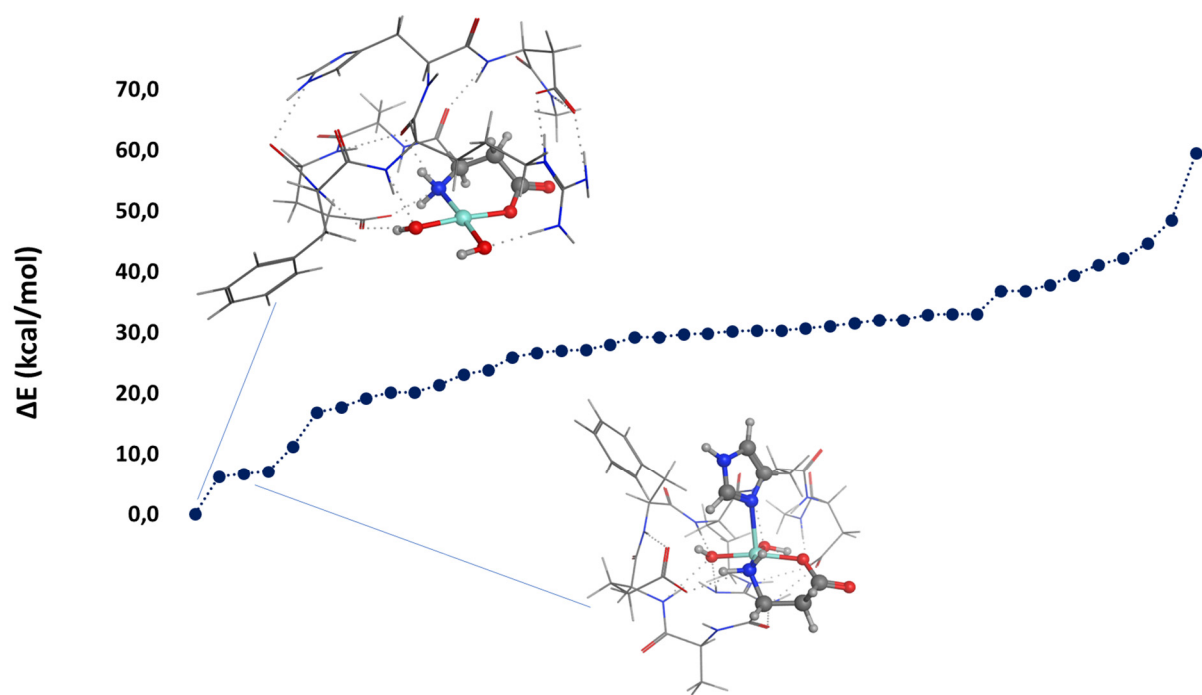
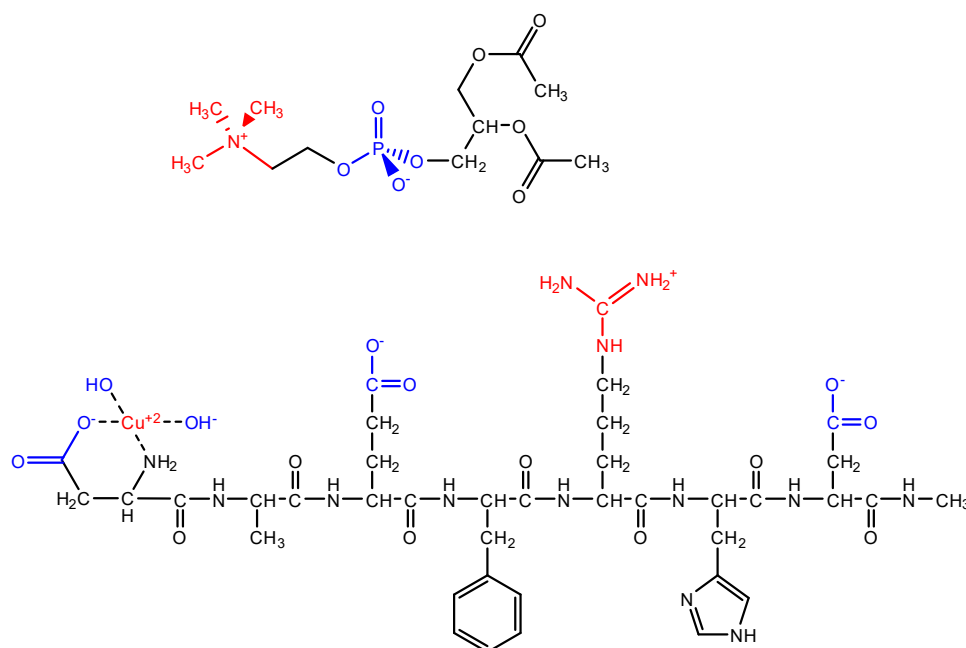


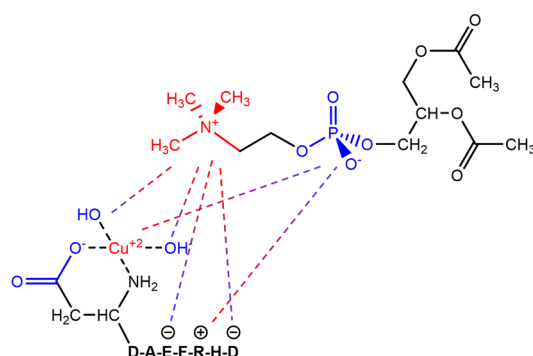
Figure S1

2. DFT Speciation and structure of $\text{Cu}(\text{OH})_2^- \cdot \text{A}\beta(1-7)$ 1-methyl 2-methyl phosphatidylcholine adducts.

In this section we report the results of the minimum energy search for the $\text{Cu}(\text{II})(\text{OH})_2^- \cdot \text{A}\beta(1-7)$ 1-methyl 2-methyl phosphatidylcholine (PN) adducts using the same approach adopted in the above section. The model considered for this search is reported below



Using molecular mechanism, we select a number of the starting point geometries to further optimized at DFT level (BP97/SV(P)/D3/COSMO=4) considering the following scheme as a guide for the MM minimum search. In particular we focus on the charge-charge non bonded interactions among Cu^{2+} and Arg side chain with $-\text{N}(\text{CH}_3)_3^+$ quaternary ammonium cations and the PO_4^- anion.



Before commenting the table with the results, we consider here the trends in the stability of the structure identified. In general, we found that the charge of the amino quaternary group is particularly shielded by methyl groups and therefore it does not significantly interact with $\text{Cu}(\text{II})(\text{OH})_2^- \cdot \text{A}\beta(1-7)$. As uno could expect, we found several structures in which PO_4 is bound to

Cu(II) in apical position. The most stabilizing salt-bridge interaction is between PO4 and Arg5 side chain.

Table S2. DFT Optimized Cu(II)(OH)₂·Aβ(1-7) PC models. E(BP) are the total energies in hartrees. ΔE refers to the total energy difference computed with respect to the most stable isomer in kcal/mol. These ΔE values are reported in the Figure S2 below this table. Binding energy with respect to the most stable Cu(II)(OH)₂·Aβ(1-7) four- and five coordinated (BE(4) and BE(5)) are in kcal/mol. The structures are classified according to the Cu coordination number (CN) and the interaction between Arg5 guanidinium side chain with the other side chains and/or peptide bond carbonylic groups.

n	CN	Arg5	DFT Energy (Hartree)	ΔE kcal/mol	BE (4) kcal/mol	BE (5) kcal/mol
1	4	PO4,OH, E3, D7	-6429,29839	0,0	-14,8	-21,4
2	5	2PO4, 2D7, CO	-6429,296193	1,4	-13,4	-20,0
3	5	2PO4, E3, CO, NH	-6429,293711	2,9	-11,9	-18,5
4	5	2D7 OH, PO4	-6429,293093	3,3	-11,5	-18,1
5	4	PO4, OH, 2D7	-6429,29225	3,9	-11,0	-17,6
6	5	E3,D7,PO4	-6429,2899	5,3	-9,5	-16,1
7	4	E3, D7 PO4	-6429,289548	5,5	-9,3	-15,9
8	4	OH,PO4,E3,D7	-6429,28704	7,1	-7,7	-14,3
9	5	E3, 2PO4,D7	-6429,28693	7,2	-7,6	-14,2
10	4	CO, PO4,E3	-6429,286641	7,4	-7,4	-14,0
11	5	OH, D3 PO4	-6429,285777	7,9	-6,9	-13,5
12	4	2PO4, E3	-6429,284262	8,9	-5,9	-12,6
13	5	E3,PO4,OH	-6429,28397	9,0	-5,8	-12,4
14	4	2OH, E3, PO4	-6429,282712	9,8	-5,0	-11,6
15	4	2CO, E3	-6429,28237	10,1	-4,8	-11,4
16	5	E3, CO	-6429,2823	10,1	-4,7	-11,3
17	5	D7,OH,PO4	-6429,280916	11,0	-3,8	-10,5
18	4	PO4,E3,D7	-6429,280559	11,2	-3,6	-10,2
19	5	2PO4	-6429,279509	11,8	-3,0	-9,6
20	4	CO,PO4,E3	-6429,27878	12,3	-2,5	-9,1
21	4	2PO4 E3 D7	-6429,27785	12,9	-1,9	-8,5
22	4	D7,E3,OH	-6429,27764	13,0	-1,8	-8,4
23	5	2PO,2E3,D7	-6429,27759	13,1	-1,8	-8,4
24	4	2PO4, D1,D7	-6429,27567	14,3	-0,6	-7,2
25	5	PO4,OH, 2E3	-6429,27489	14,7	-0,1	-6,7
26	5	2PO4,OH,D7	-6429,274799	14,8	0,0	-6,6
27	5	2D7, OH, CO	-6429,274669	14,9	0,1	-6,5
28	5	2D7, CO,OH	-6429,27448	15,0	0,2	-6,4
29	4	2PO4	-6429,27426	15,1	0,3	-6,3
30	4	2D7, OH	-6429,27393	15,3	0,5	-6,1
31	4	PO4 CO OH D7 E3	-6429,2734	15,7	0,9	-5,7
32	4	OH, E3	-6429,2725	16,2	1,4	-5,2
33	4	2PO4, 2D7	-6429,271972	16,6	1,8	-4,8
34	4	2PO4,2D7	-6429,27176	16,7	1,9	-4,7

35	5	2PO4,2D7	-6429,271682	16,8	2,0	-4,7
36	5	2E3,PO4,D1	-6429,271215	17,1	2,2	-4,4
37	5	2PO4,E3,D7	-6429,270529	17,5	2,7	-3,9
38	4	PO4	-6429,26962	18,1	3,2	-3,4
39	5	2PO4,2OH	-6429,269439	18,2	3,4	-3,2
40	5	2PO4,D1,CO	-6429,2685	18,8	3,9	-2,7
41	5	OH,D7,PO4,E3	-6429,26629	20,1	5,3	-1,3
42	4	2D7,2PO4	-6429,266168	20,2	5,4	-1,2
44	4	2D7,2PO4,D1	-6429,263786	21,7	6,9	0,3
45	4	2PO4,2H3	-6429,2593	24,5	9,7	3,1
46	4	CO, D1, OH	-6429,2591	24,7	9,8	3,2
47	4	2D7,PO4	-6429,25857	25,0	10,2	3,6
48	4	2PO4, 3E3,E7	-6429,2582	25,2	10,4	3,8
49	5	E3,D1,D7	-6429,25508	27,2	12,4	5,8
50	4	2E3,2D7	-6429,2529	28,5	13,7	7,1
51	5	2E3,2OH	-6429,252061	29,1	14,3	7,7
52	4	OH,D1,2PO4,E3	-6429,251568	29,4	14,6	8,0
53	4	D7,2D3,PO4	-6429,251419	29,5	14,7	8,1
54	4	D1,D7,2PO4	-6429,2491	30,9	16,1	9,5
55	4	His,CO,NH,PO4	-6429,247379	32,0	17,2	10,6
56	4	2D7,E3,D1	-6429,24724	32,1	17,3	10,7
57	5	2E3,2PO4	-6429,246376	32,6	17,8	11,2
58	4	D1,D7,2PO4	-6429,24389	34,2	19,4	12,8
59	4	2PO4,2D7,D1	-6429,242543	35,0	20,2	13,6
60	4	OH,PO4,	-6429,241353	35,8	21,0	14,4
61	4	E3,D1,OH,2D7	-6429,24027	36,5	21,7	15,1
62	4	2PO4,OH;D1	-6429,23014	42,8	28,0	21,4
63	4	PO4,CO,E7	-6429,2284	43,9	29,1	22,5
64	5	2PO4,2OH	-6429,217804	50,6	35,8	29,2

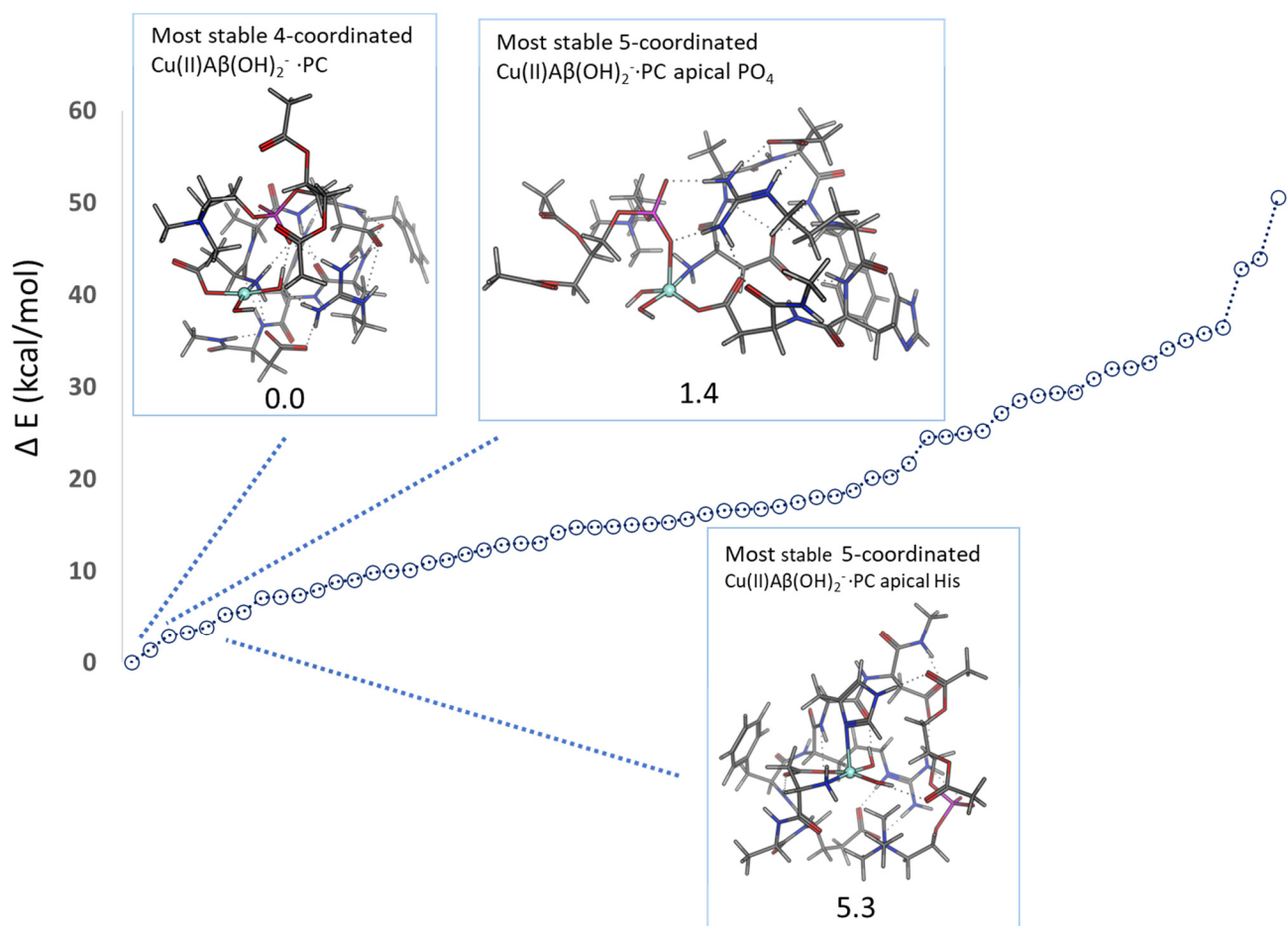


Figure S2. ΔE values of Table S2 in kcal/mol.

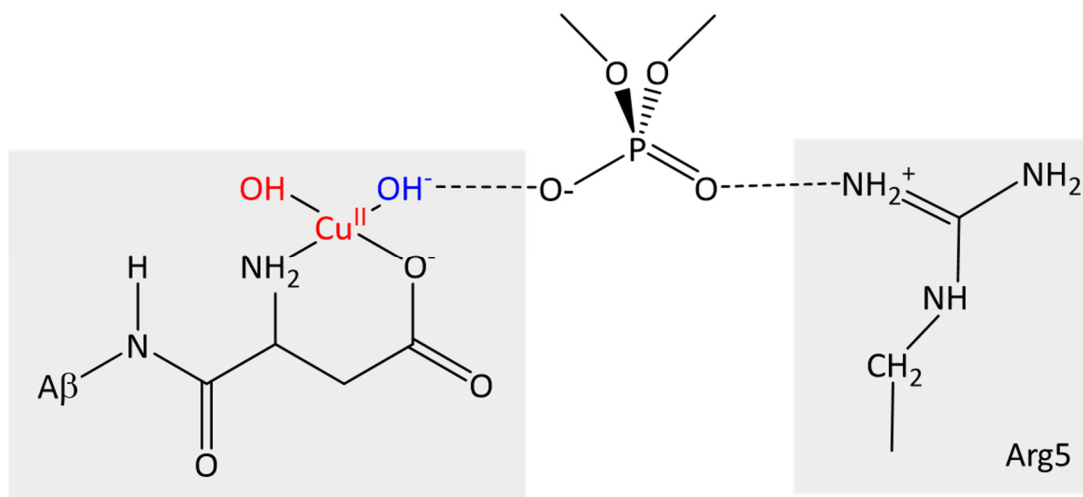


Figure S3. Salt bridge observed in structures reported in the table above between $\text{Cu(II)}(\text{OH})_2^- \cdot \text{A}\beta$ and PC through phosphate group.

3. Structures of the $\text{Cu(II)(OH)}_2^- \cdot \text{A}\beta$ fat acid chain adducts.

The four structures considered as starting point for the exploration of the $\text{Cu(II)(OH)}_2^- \cdot \text{A}\beta$ fatty acid chain PES have been obtained as follows. After a minimum search at molecular mechanics level, the best forms have been optimized at DFT level. The final adduct forms are reported below.

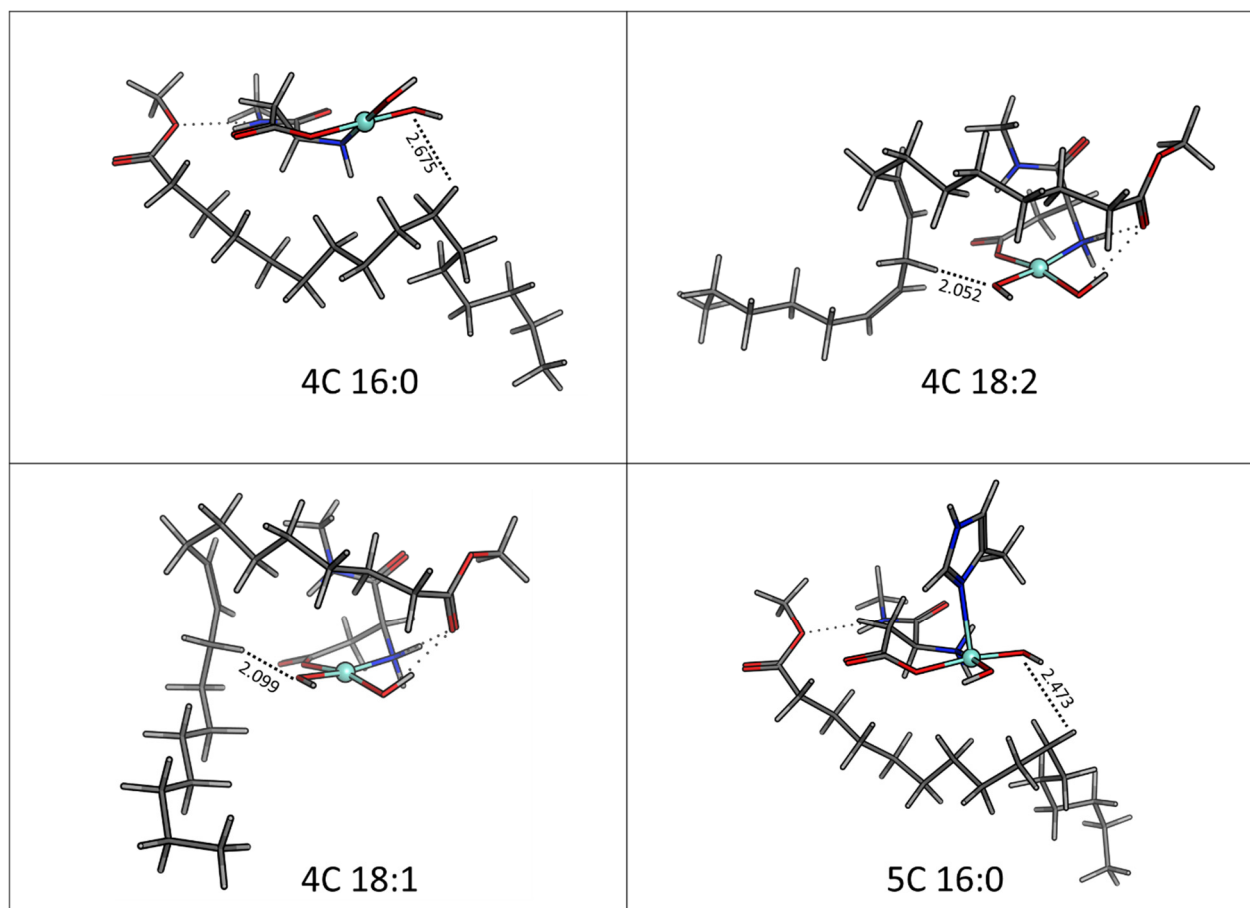


Figure S4. Structure of the most stable $\text{Cu(II)(OH)}_2^- \cdot \text{A}\beta$ fatty acid chain adducts. Distance between the hydrogen atom that belong to the C-H bond under attach and the oxygen of the OH ligand in Å.

4. NBO Spin charges of the final propagation product $\text{Cu(H}_2\text{O)(OH}^-) \cdot \text{A}\beta$ PC.

In the figures below are reported the NBO spin charges for the S=Broken symmetry solution for the six 4C final product of the OH propagation process



where are first reported values for the products of the propagation toward the head group (Figure S5) and then toward the fatty acid chains (Figure S6). Spin population is reported in electrons.

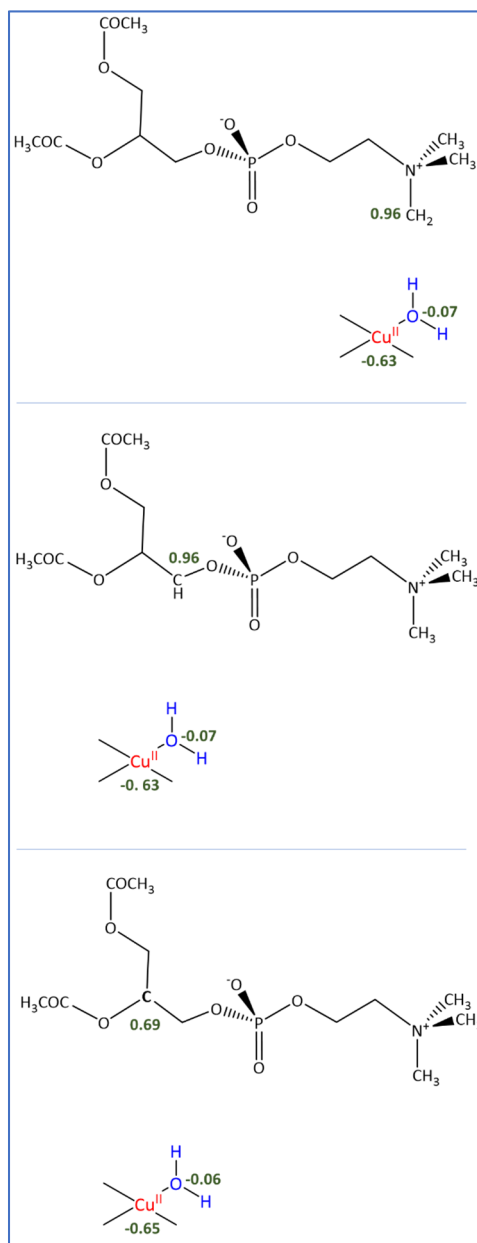


Figure S5

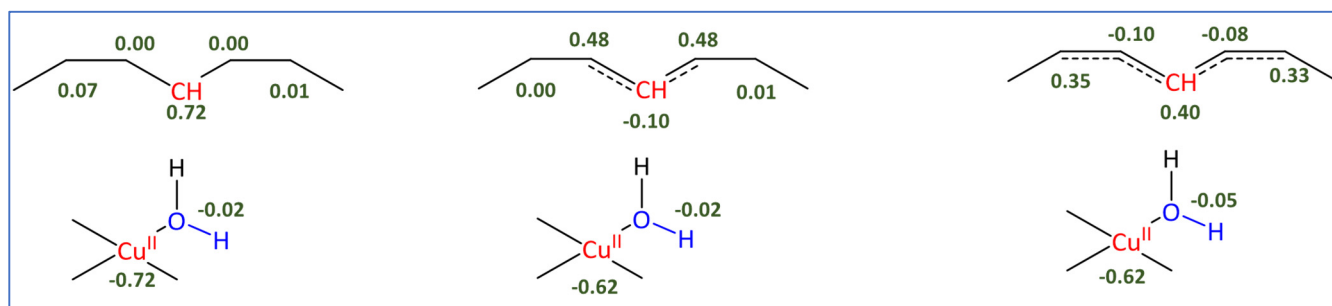


Figure S6. From left to right: S=0 broken symmetry spin population of Cu(II)(H₂O)(OH)·Aβ + PC⁺⁺ with PC equal to 16:0, 18:1 and 18:2.

5. Cu(II)(OH)_2^- A β PC PES scan of 4C and 5C in comparison.

Here are reported the PES scans along the propagation coordinate for for *sn*-2 PC position (Figure S7) and 16:0 (Figure S8) considering 4C and 5C Cu(II)(OH)_2^- A β model coordinations. In 5C the copper apical position is occupied by an imidazole ring that belong to an histidine residue.

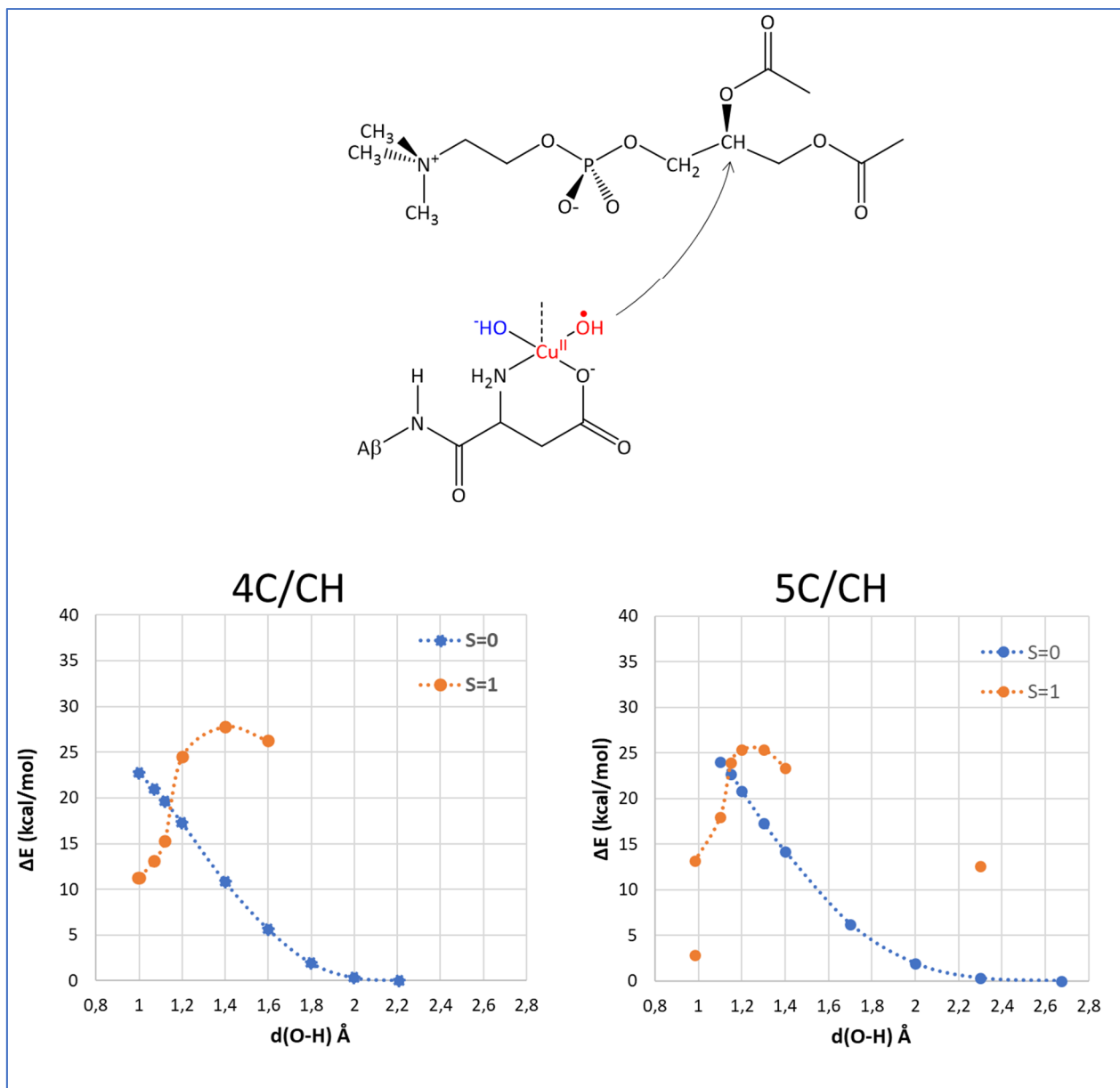


Figure S7.

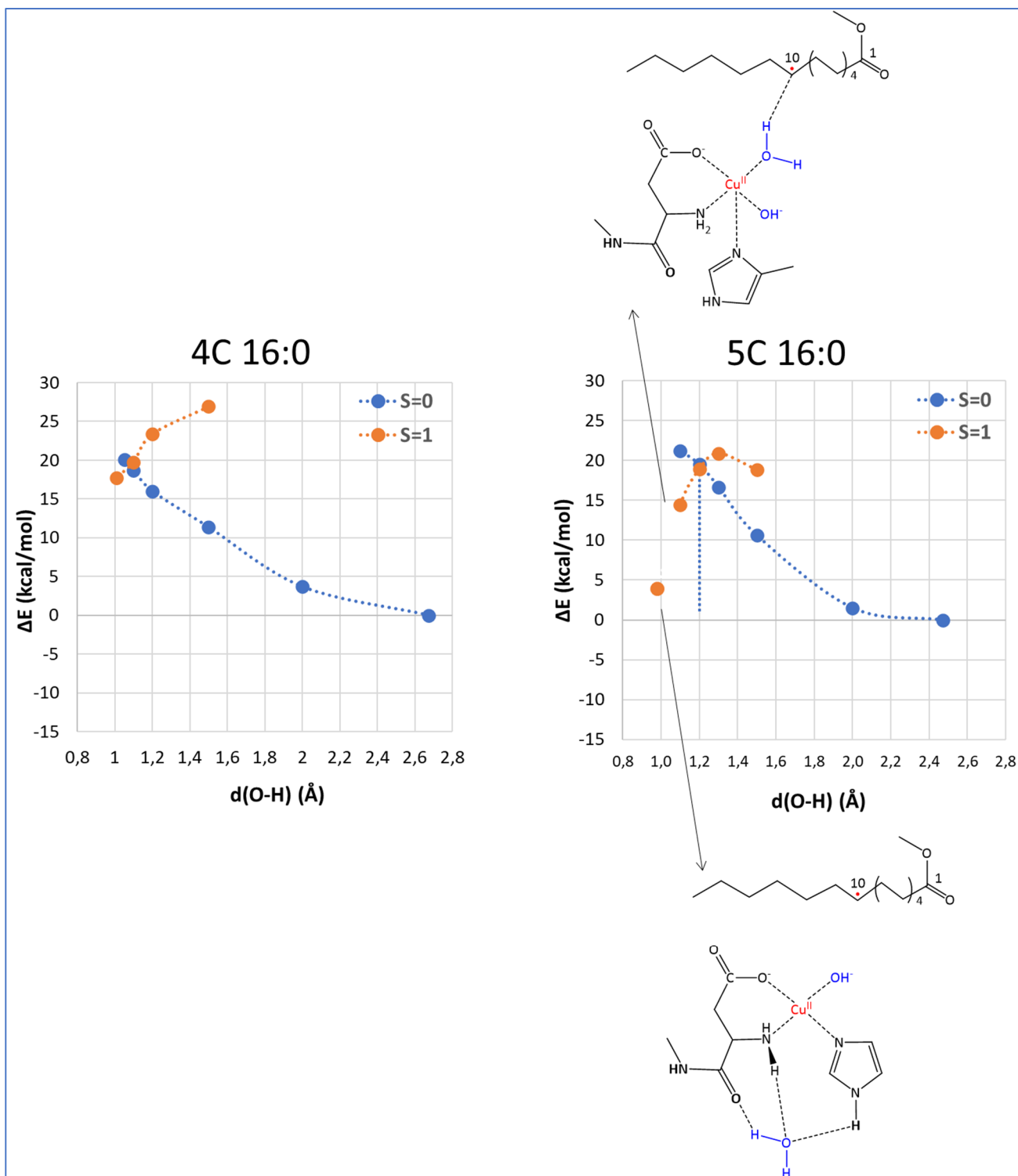


Figure S8

6. Palmitic acid 16:0 reactivity with free solvated OH radical.

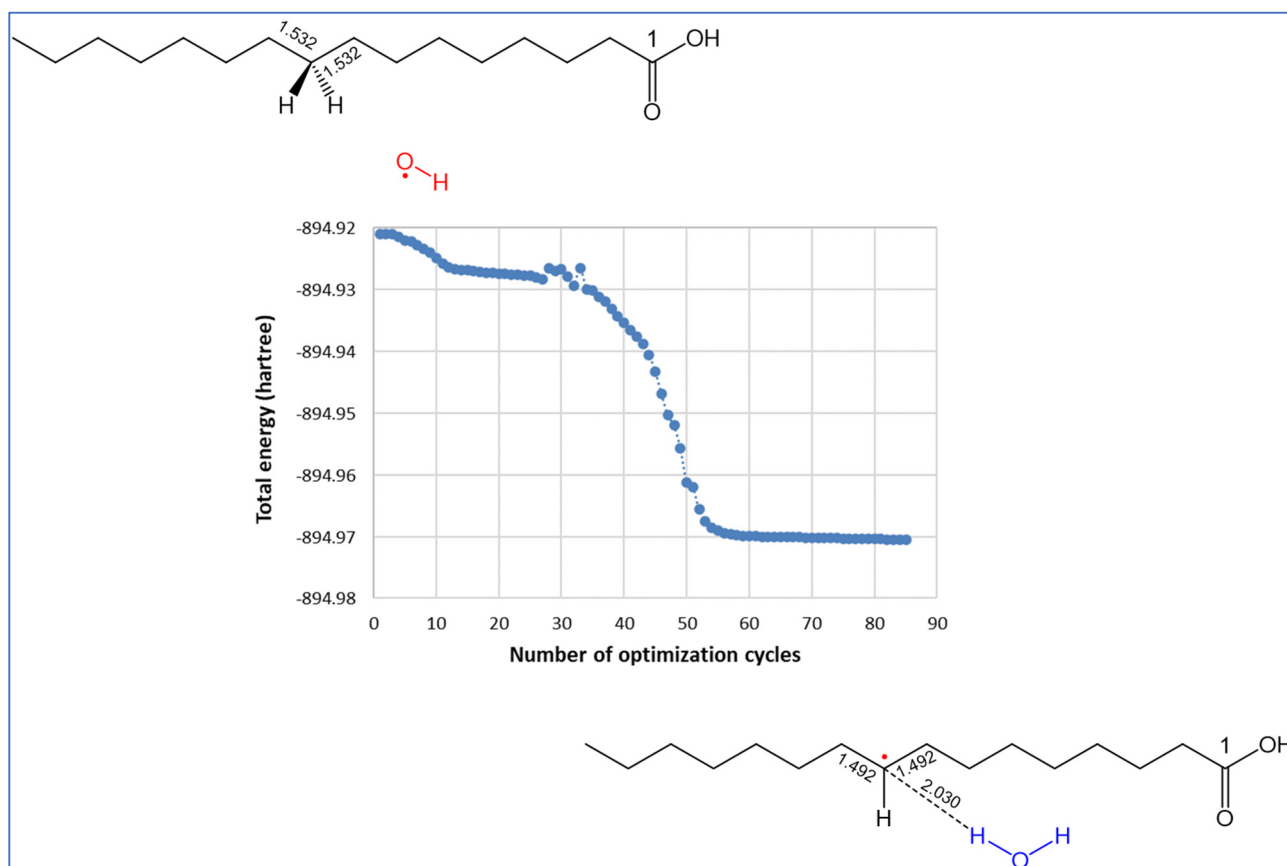


Figure S9. Energy (in hartree) history of the geometry optimization of the 16:0 palmitic acid in presence of a free OH radical. The system is a doublet state. During the DFT (BP86/def2-TZVP D3/cosmo $\epsilon=4$) optimization is observed the hydrogen abstraction from the aliphatic chain to the OH with the formation of a water molecule and a secondary carbon radical. The process of OH propagation toward the aliphatic chain is barrierless as testified by the monotonic decrease of the total energy along the geometry optimization. This plot can be compared with the PES scan for $\text{Cu(II)(OH)}_2 \cdot \text{A}\beta + 16:0$ reported on the main text (Figure 10). In this latter case the same process has an energy barrier of 16.6 kcal/mol.